

Review

# Overbank Flow, Sediment Transport, and Channel Morphology in the Lower Yellow River: A Review

Shasha Han <sup>1</sup>, Lianjun Zhao <sup>1,\*</sup>, Ao Chang <sup>2</sup>, Baichuan Liu <sup>3,\*</sup>, Jingwen Wang <sup>1,4</sup> and Jie Li <sup>5</sup>

- <sup>1</sup> Key Laboratory of Lower Yellow River Channel and Estuary Regulation, Ministry of Water Resources, Yellow River Institute of Hydraulic Research, Zhengzhou 450003, China; sshan9202@whu.edu.cn (S.H.); wangjingwen1007@whu.edu.cn (J.W.)
- <sup>2</sup> School of Water Conservancy and Transportation, Zhengzhou University, Zhengzhou 450001, China; changao0824@163.com
- <sup>3</sup> Henan Urban and Rural Planning and Design Research Institute Co., Ltd., Zhengzhou 450044, China
- <sup>4</sup> State Key Laboratory of Water Resources Engineering and Management, Wuhan University, Wuhan 430072, China
- <sup>5</sup> College of Hydraulic Science and Engineering, Yangzhou University, Yangzhou 225009, China; lij2010@whu.edu.cn
- \* Correspondence: zhaolianjun88@163.com (L.Z.); nirvana8687@126.com (B.L.); Tel.: +(86)-136-7698-0256 (L.Z.); +(86)-134-6995-9737 (B.L.)

**Abstract:** As a prerequisite and foundation for studying the evolution mechanism of river channels, an in-depth understanding of the cross-sectional morphology adjustment is required. As a starting point, it is crucial to systematically summarize and generalize the research findings on channel morphological adjustment obtained to date, particularly in the context of the significant changes in the water and sediment conditions of large rivers that have occurred worldwide. This paper provides a comprehensive review of the research findings on the three following aspects of the Lower Yellow River: the transverse distribution of overbank flow velocity, the transverse distribution of suspended sediment concentration, and the morphological adjustment of the river cross-section. There are various equations available to predict the lateral depth–average flow velocity distribution. These equations are classified into the two following categories: empirical and theoretical formulas. Theoretical formulas are obtained through consideration of the cross-sectional morphology, accounting for inertial force terms caused by secondary flow, and momentum transfer between the main channel and its floodplain. Similarly, empirical equations and theoretical formulas for sediment concentration transverse distribution are also summarized, given the different influencing factors and assumptions. We also discuss the morphological adjustment of river cross-sections based on the analysis of measured data, mathematical model calculation, and the physical model test. In particular, we propose the idea of revealing channel cross-section morphology evolution mechanisms from the theoretical level of water and sediment movement and distribution. This review aims to enhance understanding of overbank flow, sediment transport, and channel morphology in the Lower Yellow River and may also serve to some extent as a reference for the evolution and management of channels in other rivers.

**Keywords:** flow velocity; sediment concentration; transverse distribution; channel morphology; Lower Yellow River



**Citation:** Han, S.; Zhao, L.; Chang, A.; Liu, B.; Wang, J.; Li, J. Overbank Flow, Sediment Transport, and Channel Morphology in the Lower Yellow River: A Review. *Water* **2024**, *16*, 1213. <https://doi.org/10.3390/w16091213>

Academic Editor: Achim A. Beylich

Received: 11 March 2024

Revised: 17 April 2024

Accepted: 22 April 2024

Published: 24 April 2024



**Copyright:** © 2024 by the authors. Licensee MDPI, Basel, Switzerland. This article is an open access article distributed under the terms and conditions of the Creative Commons Attribution (CC BY) license (<https://creativecommons.org/licenses/by/4.0/>).

## 1. Introduction

River channels are important landforms within river systems and often affect the extensive human populations who live alongside them [1,2]. The behavior of river channels and their associated water and sediment movements are of interest to a considerable variety of engineers and scientists [3–7]. In natural settings, river channel morphology is constantly changing [8–10]. This has become more pronounced in recent decades due to the impact of climate change, the increase in human activities on the water, and the sediment

conditions of large rivers worldwide [11–15]. To gain a better understanding of how channel morphology adjusts and its complex mechanisms, it is necessary to systematically summarize the existing research results.

To study channel morphology, cross-sectional data are commonly used due to their well-established acquisition methods and accessibility in prototype surveys. An in-depth understanding of the cross-section morphology adjustment is the premise and basis for clarifying the evolutionary mechanism of river channels. Previous studies that have been conducted on channel cross-section morphology have shown that cross-sectional adjustment, such as lateral widening, narrowing, or swinging, is caused by the incompatibility of the water and sediment conditions with the channel morphology [16,17]. This is an external phenomenon that occurs due to the non-uniform distribution of flow velocity and sediment concentration in the lateral distribution, as shown in Figure 1 [18]. This non-uniform lateral distribution of water sediment leads to a non-uniform distribution of the sediment transport capacity of the flow, which may affect the lateral adjustment of the cross-section morphology. In turn, the non-uniformity of the lateral distribution of the water depth in natural rivers caused by the cross-section morphology directly leads to the non-uniformity of the lateral distribution of such additional elements as water flow velocity, sediment concentration, sediment transport capacity of flow, and riverbed deformation. In light of the complexity of water and sediment movement laws, the lateral distribution of each element is closely related and exhibits distinct quantitative characteristics. The inner mechanism of this process is very complex. It is of great significance to systematize the existing studies that have covered the level of water-sediment distribution to further promote the basic research on the adjustment mechanism of river cross-section morphology in the future.

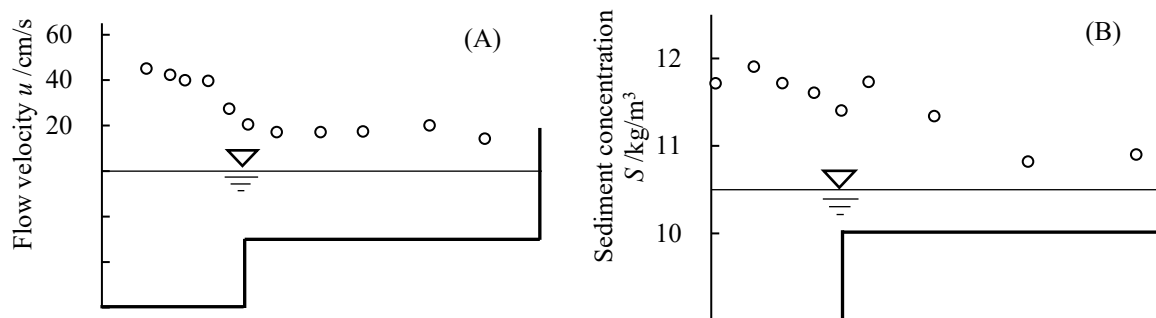


**Figure 1.** The non-uniform lateral distribution of (A) flow velocity and (B) sediment concentration. The diagram is modified from Zhao et al. [18].

The Lower Yellow River (LYR) is a typical alluvial channel, which is characterized by a high concentration of fine sediment, rapid riverbed siltation, and a drastic evolution in river regime. Ensuring flood safety for both sides of the river is important for maintaining stability and development. Two large reservoirs, Sanmenxia and Xiaolangdi, were constructed in the middle of the Yellow River to control flood risk. Sanmenxia started operating in 1960 and Xiaolangdi in 1999. Additionally, since 2002, the coordinated operation of these reservoirs has enabled the generation of artificial floods. As a result, significant changes have been observed in the water and sediment conditions of the LYR, and the channel morphology has been drastically adjusted. The Peiyu cross-section, depicted in Figure 2, offers an example of the observed changes. Between 1999 and 2018, the riverbed was scoured and the channel width increased. In recent years, since 2018, the main channel has shifted laterally, with an alternating pattern of riverbed deposition and incision. With decadal, detailed, and systematic cross-sectional data, the LYR channel provides an excellent opportunity to investigate channel morphology evolution and the associations with water and sediment movements.

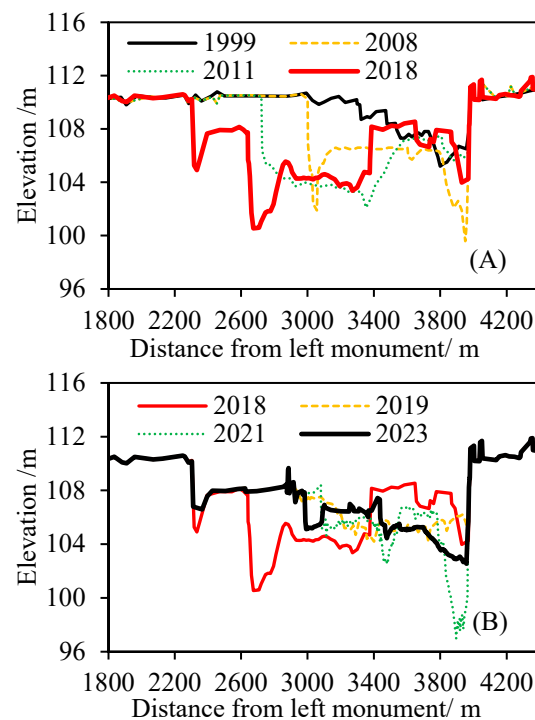


**Figure 2.** Morphological evolution of the Lower Yellow River channel from (A) 1999 to 2018 and (B) 2018 to 2023, taking the Peiyu cross-section as an example.

In this paper, we have summarized the research findings from three aspects, using the LYR as an example: the transverse distribution of depth-averaged flow velocity, the transverse distribution of suspended sediment concentration, and the morphological adjustment of the river cross-section. Based on these findings, we propose an idea to reveal the mechanism of channel cross-section morphology evolution from the theoretical level of water and sediment movement and distribution.

## 2. Transverse Distribution of the Depth-Averaged Flow Velocity

Alluvial river channels, such as the lower reaches of the Yellow River, are usually compound channels with two parts—the main channel and its floodplains. When there is a flood, the water flows over the banks and spreads out onto the floodplains. This causes energy diffusion and momentum transfer between the main channel and the floodplains, resulting in a significant difference in lateral flow velocity. An in-depth understanding of the lateral velocity distribution in compound channels is a prerequisite for many river engineering and management problems including sediment transport, vegetation, bank erosion, and so forth [19,20]. Researchers have been studying this issue since the previous century, based on physical experiments [21], mathematical models [22,23], and analytic calculations [24–27]. Analytical methods are commonly preferred due to their simplicity in practical engineering applications [20]. The current findings on analytic calculations of overbank flow in compound channels can be classified into the two following categories: empirical equations and theoretical formulas.

### 2.1. Empirical Equations for the Lateral Velocity Distribution

To predict the lateral velocity distribution in river engineering problems, previous studies have generally been based on indoor experiments or on-site measurements, analyzing the characteristics of lateral flow velocity distribution and its influencing factors, and establishing empirical equations of exponential [28–31], parabolic [32,33], and power function [34] types for the flow velocity transverse distribution. Corresponding to the three equation types above, three representative studies are listed as examples in Table 1.

**Table 1.** Some representative empirical equations of transverse depth-averaged velocity distributions in open channels.

No.	Study	Equation Type	Assumption/Sphere of Application	Derivation Processes	Main Features
(1)	Chen et al. [28]	Exponential equation	Assuming an exponential distribution of flow velocity along the channel width, and the maximum point flow velocity is located at the water surface of the thalweg.	Analyze factors that influence the distribution of flow velocity. Derive an empirical function for the lateral distribution of flow velocity that reflects water flow and cross-section morphology. Rate parameters with measured data.	Several influencing factors of lateral flow velocity distribution are considered.
(2)	Guo et al. [33]	Parabolic equation	A case study based on the measured data of Lanxi cross-section at the Fuchunjiang reservoir.	Fitting a parabolic empirical distribution function to the mean lateral flow velocity data of the cross-section with relative transverse coordinates.	Informative for overbank flow in other natural river channels.
(3)	Jiang et al. [34]	Power function equation, Equation (1)	Assuming a constant channel longitudinal slope $J$ .	Manning's formula $U = \frac{1}{n}H^{2/3}J^{1/2}$ was used to establish an empirical expression for the flow velocity at each point $U_i$ versus the cross-section's mean flow velocity $\bar{U}$ .	Simple form with some theoretical foundation.

Chen et al. [28] assumed that the flow velocity in a channel was exponentially distributed along its width, and that the maximum flow velocity occurred at the water surface of the thalweg. Based on this, they identified the water flow characteristics and cross-sectional morphology as influencing factors and developed an empirical function to describe the lateral distribution of flow velocity. The empirical function was calibrated using measured data, and it was found to have relatively high accuracy in practical applications [28]. Guo et al. [33] utilized data from the Lanxi cross-section at the Fuchunjiang reservoir to fit a parabolic empirical distribution function to the mean lateral flow velocity data of the cross-section, based on relative transverse coordinates. This finding can be informative for researchers studying lateral flow velocity in natural channels. Moreover, it is common practice to assume a constant channel longitudinal slope  $J$  and to use Manning's formula  $U = \frac{1}{n}H^{2/3}J^{1/2}$  to develop an empirical expression for the flow velocity at each point  $U_i$  versus the cross-section mean flow velocity  $\bar{U}$  as follows [34]:

$$\frac{U_i}{\bar{U}} = c_1 \frac{\bar{n}}{n_i} \left( \frac{H_i}{\bar{H}} \right)^{2/3} \quad (1)$$

where  $\bar{n}$  and  $n_i$  are the cross-section's average roughness and the roughness at each point, respectively;  $\bar{H}$  and  $H_i$  are the cross-section's average water depth and the depth at each point, respectively; and  $c_1$  is a cross-section morphology coefficient, and it can be provided based on the mass conservation law as follows:

$$c_1 = \frac{\bar{Q}}{\int_{y_2}^{y_1} \frac{\bar{n}}{n_i} \frac{\bar{U}}{H^{2/3}} H_i^{5/3} dy} \quad (2)$$

where  $\bar{Q}$  is the cross-section's average flow rate;  $y$  is the lateral coordinate; and  $y_1$  and  $y_2$  are the starting point and the endpoint of the cross-section ( $y_2 > y_1$ ). Equation (1) ignores the intermixing and exchange between water bodies in the transverse direction.

Empirical formulas are generally easier to use in practical applications. However, they do not have a theoretical basis and also have flaws such as the mismatched dimensions in Equations (1) and (2). For this reason, there have been many theoretical studies conducted on the transverse distribution of overbank flow velocity.

## 2.2. Theoretical Formulas for the Lateral Velocity Distribution

To predict the lateral variation in overbanks in compound channels, various analytical models have been proposed by different scholars, such as the coherence method [25], the channel–floodplain water–sediment exchange model [27,35,36], the SKM method [24], etc. The coherence method is considered the best one-dimensional method for dealing with overbank flow and its associated complex roughness and cross-sectional shape problems [37]. The channel–floodplain water–sediment exchange model and the SKM method represent the development of the one-dimensional method into a two-dimensional method, which can describe the phenomenon of overbank flow more accurately and in greater detail [26]. The text below provides a review of the lateral velocity distribution methods, mainly focusing on quasi-2D methods, and Table 2 shows some representative theoretical findings.

### (1) Theoretical background

These quasi-2D models are based on the depth-averaged or depth-integrated form of the Navier–Stokes equations. For the case of steady uniform flow in a straight channel, the equations are reduced to a single equation, which describes the lateral distribution of depth-averaged velocity of unit flow across a channel. To obtain analytical solutions for the lateral distributions of depth-averaged velocity, the depth-averaged momentum equation for the streamwise motion of a fluid element in an open channel is combined with the continuity equation, and for constant homogeneous flow the equation is as follows:

$$\rho \left[ \frac{\partial}{\partial y} (UV) + \frac{\partial}{\partial z} (UW) \right] = \rho gJ + \frac{\partial}{\partial y} \left( -\rho \overline{u'v'} + \mu \frac{\partial U}{\partial y} \right) + \frac{\partial}{\partial z} \left( -\rho \overline{u'w'} + \mu \frac{\partial U}{\partial z} \right) \quad (3)$$

where  $x$ ,  $y$ , and  $z$  are streamwise parallel to the channel and lateral and normal to the bed, respectively, as shown in Figure 3.  $U$ ,  $V$ , and  $W$  are the average velocity components in the  $x$ ,  $y$ , and  $z$  directions, respectively, and  $u'$ ,  $v'$ , and  $w'$  are the turbulent velocity components in the  $x$ ,  $y$ , and  $z$  directions, respectively.  $\rho$  represents the fluid density;  $\mu$  is the fluid viscosity coefficient;  $J$  is the channel bed slope; and  $g$  is the gravitational acceleration. Assuming that the channel bed slope  $J$  and the roughness  $n$  remain constant across the channel's width, Equation (3) physically means that secondary flows = weight force + Reynolds stresses of the lateral ( $x$ – $y$ ) plane and vertical ( $x$ – $z$ ) plane.

### (2) Studies mainly focusing on the momentum transfer between the main channel and its floodplain

Various models for the lateral distribution of flow velocity have been proposed, based on the integration of Equation (3) over the flow depth. One of the most notable models in China for an overbank flood is the channel–floodplain water–sediment exchange model, which was the proposal of the scholars Zhou [35], Chen et al. [36], and Ji and Hu [27]. The idea is to create a generalization of the river's cross-section by using a compound rectangular channel. Based on the characteristics of the overbank flow movement, the compound cross-section can be divided into the three following zones: the boundary zone (I), the undisturbed zone (II), and the interactive zone between the main channel and its floodplain (III), as shown in Figure 3. For each area, a formula for the transverse eddy viscosity coefficient is established, which helps derive the lateral distribution of the flow velocity.

It is widely accepted that zone I is of a relatively small size, while the water flow in zone II has one-dimensional characteristics and is not greatly affected by the exchange in momentum between the main channel and floodplain. The transverse eddy viscosity coefficient in zone II can be determined using the formula  $\bar{\epsilon}_{yx} = 0.134U_*H$ , which considers the shear velocity  $U_*$  and the water depth  $H$  [38]. In contrast, the flow in zone III displays strong three-dimensional characteristics, and the lateral variation in the flow velocity is significant. This makes the lateral distribution of the flow velocity in zone III a challenging and complex issue for scholars to study.

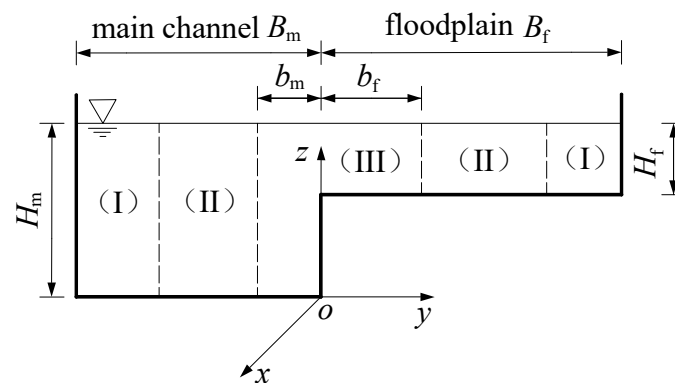


**Figure 3.** Division of the compound rectangular channels of overbank flow. Notation:  $B_m$ ,  $B_f$  = semi-width of the main channel and the floodplain, respectively;  $b_m$ ,  $b_f$  = width of the main channel and floodplain in the interactive zone between the main channel and floodplain (zone III), respectively;  $H_m$ ,  $H_f$  = water depth in the main channel and the floodplain, respectively; zones I, II, and III are the boundary zone, the undisturbed zone, and the interactive zone between the main channel and its floodplain, respectively. The sketch is redrawn from Figure 2 of Zhou [35].

Zhou [35] assumed that the inertial force caused by the secondary flow can be overlooked. This implies that the left-hand side of Equation (3) is equal to zero. Based on this assumption, a differential equation for the transverse eddy viscosity coefficient was derived. The theoretical formula for the lateral depth-averaged flow velocity distribution in zone III can then be obtained using the measured data.

The assumption that the inertial force caused by the secondary flow can be neglected makes the derivation of the analytical solution of the equations relatively easy. So many scholars have completed related studies based on this assumption, and only the specific treatment methods for momentum transfer between the main channel and its floodplain are different. Some studies neglected the inertial force term of the secondary flow, but considered the influence of other factors on the lateral distribution of flow velocity. For example, Zong et al. [39] considered the floodplain transverse slope in the derivation of the lateral distribution of flow velocity. Based on the Boussinesq assumption and the Darcy–Weisbach formula, the motion equation considering the floodplain transverse slope was derived. Using the measured data of water depth in the Lower Yellow River, the cross-section morphology is generalized as shown in Figure 4 and the transverse eddy viscosity coefficient equation is fitted. Finally, an analytical solution for the lateral depth-averaged velocity distribution of overbank flow on the floodplain transverse slope is provided.

However, practical analysis reveals that the secondary flow generates a non-zero inertial force. Several studies have explored the secondary flow inertial force, with different assumptions generated in each research study. For instance, Ji and Hu [27] assumed that the secondary flow inertial force was proportional to the gravitational component of the water flow. Based on this assumption, they used the simplified water kinematic equation and sediment diffusion equation to derive the expression for the transverse eddy viscosity coefficient. Through a combination of Bessel's equation solution with superposition, an analytical solution for the distribution of the lateral depth-averaged velocity in zone III was obtained.

To summarize, the studies mentioned above have either neglected the inertial force term produced via the secondary flow or have accounted for it in a simple manner. Here, the main focus lies on the impact of momentum exchange between the main channel and its floodplain in zone III. The expression for the coefficient of transverse eddy viscosity is provided via various techniques and boundary conditions. Through utilization of the method of coefficients, analytical solutions for the lateral depth-averaged flow velocity distribution in zone III can be derived.

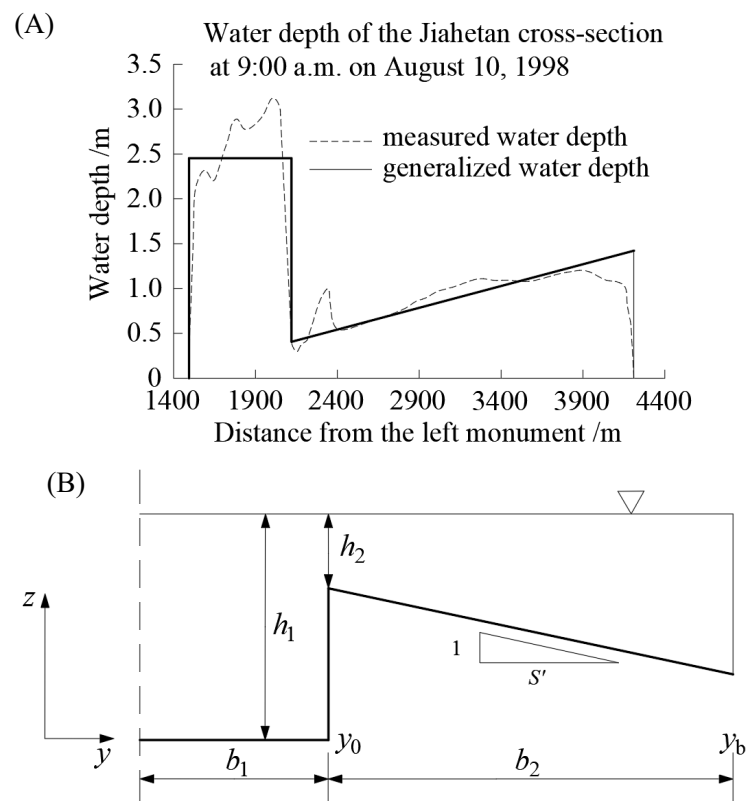


**Figure 4.** The generalization of (A) the water depth and (B) the cross-section morphology in the Lower Yellow River, based on measured data for the Jiahetan cross-section. Notation:  $S'$  = floodplain transverse slope;  $b_1, b_2$  = semi-width of the main channel and the floodplain, respectively;  $h_1$  = water depth in the main channel and the floodplain;  $h_2$  = minimum water depth in the floodplain;  $y_0, y_b$  are the left and right sides of the floodplain, respectively. The sketch is redrawn from Figures 1 and 2 of Zong et al. [39].

### (3) Studies mainly focusing on the effect of secondary flows

In contrast to focusing on the momentum transfer impact in zone III, there is another class of studies that have focused on the effect of secondary flow on the lateral distribution of flow velocity. They generally agree on the transverse eddy viscosity coefficient  $\bar{\epsilon}_{yx} = \lambda U_* H$  across the cross-section; however, different assumptions are made on the secondary flow term (Table 2, from no. 3 to no. 4). For example, Wu et al. [40] suggested that the inertial force caused by the secondary flow is related to the water gravity and boundary shear stress. They analyzed the forces acting on the compound channel flows and obtained a model for transverse flow velocity. Using the difference method, an analytical solution for the lateral depth-averaged flow velocity distribution was deduced.

Another widely used analytical model for predicting the lateral distribution of flow velocity in open channels is the SKM model, proposed by Shiono and Knight [24]. This model has been proven to produce satisfactory results for channels with both a simple and compound cross-section morphology (Figure 5). Unlike the three-zone division shown in Figure 3, the SKM model divides the cross-section into the two following regions, a region of constant depth and a region with a linearly varying side bed (1:s, vertical/horizontal), as shown in Figure 5. The analytical solution for the lateral distribution of the flow velocity differs in each region.

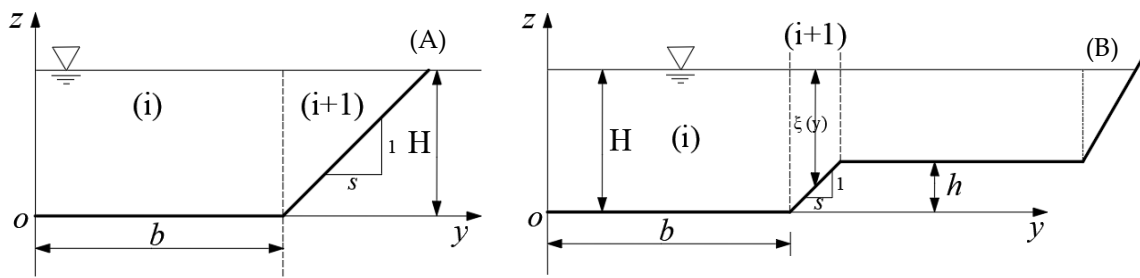


**Figure 5.** A sketch of (A) the simple channel and (B) the compound trapezoidal channel. Notation: (i) represents the region of constant depth; (i + 1) represents the region with a linearly varying side bed;  $s$  = the channel side slope of the banks;  $H$  = the water depth;  $h$  = the depth displacement of main channel and its floodplain.  $\zeta$  is the local depth given by  $\zeta = \begin{cases} H - (y - b)/s & y > 0 \\ H - (y - b)/s & y < 0 \end{cases}$ . The sketch is redrawn from Figures 1 and 2 in the study of Tang and Knight [19].

To obtain the depth-averaged velocity equation, the SKM model integrates Equation (3) over the flow depth; therefore, it follows that

$$\frac{\partial}{\partial y} [H(\rho UV)_d] = \rho g H J + \frac{\partial H \bar{\tau}_{yx}}{\partial y} - \tau_b \left(1 + \frac{1}{s^2}\right)^{1/2} \tag{4}$$

where the bed shear stress  $\tau_b = \rho \frac{8}{f} U_d^2$ ; the depth-averaged lateral shear stress  $\bar{\tau}_{yx} = \rho \bar{\epsilon}_{yx} \frac{\partial U_d}{\partial y}$ ; the transverse eddy viscosity coefficient  $\bar{\epsilon}_{yx} = \lambda U_* H$ ; the shear velocity  $U_* = \sqrt{\tau_b / \rho}$ ; and  $\lambda$  = dimensionless eddy viscosity. Equation (4) can be rewritten as follows:

$$\frac{\partial}{\partial y} [H(\rho UV)_d] = \rho g H J + \frac{\partial}{\partial y} \left\{ \rho \lambda H^2 \left(\frac{f}{8}\right)^{1/2} U_d \frac{\partial U_d}{\partial y} \right\} - \rho \frac{8}{f} U_d^2 \left(1 + \frac{1}{s^2}\right)^{1/2} \tag{5}$$

Assuming the lateral distribution of  $[H\rho UV]_d$  is linear in the main channel and its floodplain, i.e., the transverse gradient of secondary flow term  $\Gamma = \frac{\partial}{\partial y} [H(\rho UV)_d]$  is constant, an analytical solution of Equation (5) can be obtained.

Nevertheless, Tang and Knight [19] re-examined the SKM model; they found that the original SKM model does not meet the no-slip boundary condition, which mainly results from the assumption of a linear relationship for the  $[H\rho UV]_d$  distribution. To overcome this issue, they assumed  $\Gamma^* = \frac{\partial}{\partial y} [(\rho UV)_d] = \frac{\partial \Psi}{\partial y}$ . In addition, a further, simpler model used by Abril and Knight [41] assumes  $\Gamma = H\Gamma^*$ .

All the SKM models mentioned above provide the same analytical solution for the constant depth region. However, variations exist for the region where the side bed varies linearly. A comparison conducted by Tang and Knight [19] showed that all SKM models can generate velocity distributions that are consistent with the available data.

Based on the SKM method, many scholars have proposed analytical models for the lateral distribution of flow velocity in open channel flow with their own characteristics. For instance, Wark et al. [42] used the discharge intensity form of the lateral distribution equation, and proposed a method for flow velocity lateral distribution which was akin to the SKM method [24], except that the secondary flow term  $\Gamma$  was ignored. Ervine et al. [43] assumed that the time-averaged flow velocities  $U$  and  $V$  were proportional to the depth-averaged streamwise velocity  $U_d$  ( $U = k_1 U_d, V = k_2 U_d$ ), and the inertial force term caused by the secondary flow could be reduced to a simpler form,  $\partial (H\rho K' U_d^2) / \partial y$ . Consequently, an analytical model could be obtained.

**Table 2.** Some representative theoretical findings of quasi-2D methods for the transverse distribution of depth-averaged velocity.

No.	Study	Channel Type	Regions of Concern	Assumptions on the Effect of Secondary Flows	Assumptions on the Momentum Transfer between Main Channel and Its Floodplain, Transverse Eddy Viscosity Coefficient ( $\bar{\epsilon}_{yx}$ )
(1)	Zong et al. [39]	Compound channels (Figure 4).	The channel floodplain with a transverse slope.	The inertial force term caused by the secondary flow has been neglected.	The motion equation considering the floodplain transverse slope is derived. Using measured data of cross-section, the equation of $\bar{\epsilon}_{yx}$ is fitted.
(2)	Ji and Hu [27]	Compound rectangular channels (Figure 3).	The interactive region between the main channel and its floodplain (zone III).	Assuming the inertial force term caused by the secondary flow is proportional to the gravitational component of the water flow.	Using the simplified water kinematic equation and sediment diffusion equation, the expression for $\bar{\epsilon}_{yx}$ is deduced.
(3)	Wu et al. [40]	Compound rectangular channels (Figure 3).	The whole cross-section.	Assuming the inertial force term caused by the secondary flow is related to the water gravity and boundary shear stress.	$\bar{\epsilon}_{yx} = \lambda U_* H$
(4)	Shiono and Knight [24]	Simple and compound trapezoidal channels (Figure 5).	The whole cross-section.	The transverse gradient of secondary flow term $\Gamma = \frac{\partial}{\partial y} [H(\rho UV)_d]$ is constant.	$\bar{\epsilon}_{yx} = \lambda U_* H$
(5)	Ervine et al. [43]	Simple and compound trapezoidal channels.	The whole cross-section.	Assuming the time-averaged flow velocities $U$ and $V$ are proportional to the depth-averaged streamwise velocity.	-

In general, many theoretical studies on the lateral distribution of flow velocities start with the Navier–Stokes equations. Some studies have ignored or simplified the secondary flow term and have instead focused on the momentum exchange in the interaction zone between the main channel and its floodplain. Others have assumed the transverse eddy viscosity coefficient  $\bar{\epsilon}_{yx} = \lambda U_* H$  and mainly focused on the secondary flow term. Several studies have found that the transverse eddy viscosity coefficient has less influence on the results than the secondary flow term for overbank flows; however, it remains crucial for inbank flows [19,44]. Even though various theoretical formulations of the lateral distribution of flow velocities have focused on different terms, they provide multiple options for studying the lateral distribution of flow velocities under different flow conditions.

Many researchers have also extensively studied three hydraulic parameters related to the bed friction factor  $f$ , lateral eddy viscosity  $\lambda$ , and secondary flow term  $\Gamma$  in the SKM method for various cases [41,45–52].

Additionally, the SKM method has been extensively tested and its applicability is constantly expanding to various channel morphologies, floodplain characteristics, and channel zoning [53–58]. For instance, McGahey et al. [53] investigated the practical application of the SKM method to natural rivers. Rezaei and Knight [54] explored the possibility of using the SKM method to predict depth-averaged velocity and boundary shear stress in

compound channels with non-prismatic floodplains, and for this reason, the SKM method was modified. Alawadi et al. [52] and Alawadi and Tumula [55] applied the SKM method in asymmetric compound channels. Although not covered in this review, the SKM method has also been widely used in studies concerning the hydrodynamic characteristics of water flow in vegetation channels [59–63].

### 3. Transverse Distribution of the Suspended Sediment Concentration

Contrary to the studies of flow velocity distributions, the transverse distribution of suspended sediment concentration has received much less attention. This is because measuring sediment data accurately in rivers and experiments is challenging. However, in overbank flows, there is a significant difference in flow velocities across river cross-sections, and the suspended sediment concentration is also unevenly distributed laterally. This may cause different levels of scouring and siltation changes at various locations of the river cross-section. The research on the transverse distribution of the suspended sediment concentration can be classified into the two following categories: empirical and theoretical formulas. Some representative results of this research are presented in Table 3.

**Table 3.** Some representative findings of research on the transverse distribution of suspended sediment concentration.

Equation Type	Representative Findings	Assumptions/Sphere of Application	Derivation Processes	Main Features
Empirical equations	Gao et al. [64]	Considering the effects of hydraulic factors.	Analyze the factors that affect lateral distribution of the suspended sediment concentration. Propose a form of its expression, and fit the coefficients based on measured data. Afterward, establish an empirical equation for the lateral distribution of suspended sediment concentration.	The equations are straightforward in structure and easy to apply, but they are constructed with a single factor in mind.
	Wei et al. [65] Zhang [66]	Considering the effects of stream discharge and sediment transport capacity.		
	Zhao et al. [67] Jiang et al. [34]	Introducing a suspension index to reflect the effect of suspended sediment composition.		
Theoretical formulas	Chen et al. [68] Ji and Hu [27]	Compound rectangular channels (Figure 3). Assuming that the river channel is in equilibrium, and the lateral diffusion coefficient is equal to the transverse eddy viscosity coefficient.	Using the channel–floodplain water–sediment exchange model, the analytical solution for the lateral distribution of suspended sediment concentration in zone III is deduced, using the method of coefficients to be determined.	Flowing water in natural rivers has varying sediment capacities across its cross-section. As a result, the assumption that the main channel and its floodplain are in an equilibrium state of erosion and siltation simultaneously is not accurate in reality.

#### 3.1. Empirical Equations for the Lateral Suspended Sediment Concentration Distributions

Several studies have aimed to establish a reliable equation that can predict the lateral distribution of suspended sediment concentration in practical scenarios. The approach involves analyzing the factors that influence the lateral distribution of suspended sediment concentration, and then proposing an equation with coefficients determined from the measured data. For example, Gao et al. [64] considered the effects of hydraulic factors on the lateral distribution of suspended sediment concentration, and identified an expression that contains unknown coefficients. They then fit these coefficients based on measured data, and an empirical equation for the lateral distribution of suspended sediment concentration was obtained.

Wei et al. [65] and Zhang [66] investigated the impacts of stream discharge and sediment transport capacity on lateral sediment concentration distributions, and proposed

an empirical relationship between the sediment concentration at each point and the cross-sectionally averaged sediment concentration.

Furthermore, other scholars have proposed empirical equations with specific characteristics for the lateral distribution of suspended sediment concentrations [69,70]. These empirical equations possess a relatively simple structure that makes them more convenient for practical applications such as numerical modeling calculations. However, it is important to note that empirical equations may not fully capture the lateral variability in sediment concentration.

Zhao et al. [67] and Jiang et al. [27] discovered that the lateral distribution of sediment concentration is not only under the influence of hydraulic factors and sediment concentration, but also of the impact of suspended sediment composition. Based on the analysis of a substantial volume of measured data in the Lower Yellow River, a suspension index  $\omega_s/\kappa U_*$  was introduced to effectively capture the influence of suspended sediment composition on the lateral distribution of sediment concentration. Furthermore, a formula for accurately predicting the lateral distribution of sediment concentration was developed, which is applicable to both inbank and overbank flows. The formula is presented as follows:

$$\frac{S_i}{\bar{S}} = c_2 \left( \frac{H_i}{\bar{H}} \right)^{(0.1 - 1.6 \frac{\omega_s}{\kappa U_*} + 1.3 S_V)} \left( \frac{U_i}{\bar{U}} \right)^{(0.2 + 2.6 \frac{\omega_s}{\kappa U_*} + S_V)} \quad (6)$$

where  $c_2$  is a coefficient which can be determined using measured data.  $\bar{S}$ ,  $\bar{H}$ , and  $\bar{U}$  are the cross-sectionally averaged sediment concentration, water depth, and flow velocity, respectively, and the sediment concentration, water depth, and flow velocity at each point of the cross-section are denoted as  $S_i$ ,  $H_i$ , and  $U_i$  correspondingly.  $\omega_s$  is the sediment settling velocity;  $\kappa$  represents the Karman constant; and  $S_V$  is the sediment concentration by volume. Equation (6) is more comprehensive in its consideration of factors, ease of application, and has a certain universality in the Lower Yellow River, but its mechanism is somewhat inadequate.

### 3.2. Theoretical Formulas for the Lateral Suspended Sediment Concentration Distributions

For a constant uniform flow, the lateral distribution of suspended sediment concentration in theoretical studies can be described using the sediment diffusion equation as follows:

$$\frac{\partial}{\partial y} \left( \varepsilon_{sy} \frac{\partial S}{\partial y} \right) + \frac{\partial}{\partial z} \left( \varepsilon_{sz} \frac{\partial S}{\partial z} + \omega_s S \right) = \frac{\partial S}{\partial t} \quad (7)$$

where  $S$  is the sediment concentration;  $\varepsilon_{sy}$ , and  $\varepsilon_{sz}$  are the lateral and vertical sediment diffusion coefficients, respectively; and  $\omega_s$  represents the sediment settling velocity. The temporal variation in suspended sediment concentration within a given cross-section is governed by gravity and turbulence diffusion, both horizontally and vertically, as described in Equation (7).

In the same way that lateral velocity distribution has been theorized, the current examination of suspended sediment concentration distribution in the transverse direction also relies on the fundamental concepts of the channel–floodplain water–sediment exchange model mentioned previously. Through the assumption of an equilibrium state of longitudinal sediment transport under uniform flow conditions, Equation (7) can be simplified via setting its right-hand side to zero. Integrating Equation (7) over the flow depth and simplifying it appropriately based on the assumption that the lateral diffusion coefficient equals the transverse eddy viscosity coefficient, the analytical solution for the transverse distribution of the suspended sediment concentration in the interactive region between the main channel and its floodplain (zone III in Figure 3) can be determined using the method of coefficients [27,68].

In summary, researchers have examined several theoretical formulas that offer potential methods for predicting suspended sediment concentration distribution in practical settings. However, it is important to note that the sediment capacity of natural rivers can vary

across their width; the assumption that the main channel and floodplain are in a state of simultaneous erosion and siltation equilibrium is not entirely accurate in real-life scenarios, i.e., see the right-hand side of Equation (7),  $\partial S/\partial t \neq 0$ . This highlights the need for further study and for attention to be paid to the distribution of lateral sediment concentration. Additionally, it should be mentioned that some effects caused by high sediment concentrations, including turbulence damping, sediment-induced density stratification, hindered settling, fluid mud, hindered erosion, etc., have not been considered in the previous theoretical studies. However, these effects are prominent in highly concentrated flows, such as the heavily sediment-laden floods that sometimes occur in the LYR.

#### 4. Studies on the Morphological Adjustment of Channel Cross-Section in the LYR

The LYR's channel evolution has been a topic of fascination for researchers due to its unique characteristics, such as a high concentration of fine sediment, rapid siltation of the riverbed, and drastic changes in river regime. To better understand how the LYR channel morphology has changed, researchers have approached the topic under study in different ways. Some have focused on the microscopic mechanisms of water and sediment movement, while others have taken a macroscopic approach to uncover the laws governing channel cross-sectional adjustment.

Numerous investigations have been conducted to study the cross-sectional morphology in the LYR; accordingly, there are two main categories of research. One approach involves analyzing the measured data to calculate the parameters of channel morphology characteristics at different spatial and temporal scales, such as the main channel area, river width, water depth, and river phase. Then, empirical relationships are established between these parameters and their influencing factors [71–79]. For example, Li [80] calculated the channel morphology characteristic parameters in three different periods based on the measured data: the period of Sanmenxia Reservoir operation (1973–1986), the period of low flow and reduced sediment (1986–1999), and the period of Xiaolangdi Reservoir operation (1999–2016). The relationship between each parameter and water and sediment conditions in flood and non-flood periods was then established. Xia et al. [81] investigated the change process on a cross-sectional scale and sectional scale of bankfull river width in the wandering reaches of the LYR after the operation of the Xiaolangdi Reservoir, and established its empirical relationship with the average fluvial erosion intensity. Li et al. [74] studied the process of river regime adjustment in the LYR and concluded that under the continuous low-concentrated flow released from the Xiaolangdi Reservoir, the wandering reach channel showed an increased river width, a scattered river regime, increased in-channel bars, and more apparent abnormal bends. These studies typically involve qualitative analyses or semi-quantitative calculations, making them ideal for exploring large-scale and long-term patterns of river channel evolution.

Another research approach involves utilizing mathematical or physical models to simulate river bed deformation. Water–sediment mathematical models, both one-dimensional and two-dimensional, are commonly used, but they have limitations in accurately representing the lateral deformation of river channels [82–84]. Even with special treatment of the plane two-dimensional model via coupling of both the longitudinal and lateral riverbed deformation modules, they can only simulate bed evolution and bank deformation, without the ability to calculate the detailed adjustment process of the river cross-section morphology [85–88]. Therefore, many researchers have opted to use physical models to study the changes in river cross-sections. For example, Wang et al. [89] utilized physical modeling experiments to investigate the changes in the cross-section morphology of wandering reach in the LYR under various sediment-laden flow conditions. The research revealed that a narrow and deep channel was easily formed with the highly sediment-laden flow; however, maintaining this cross-section morphology for an extended period in a compound channel was challenging. Zhang [90] studied cross-section adjustment patterns in the LYR by conducting a constant water–sediment generalization model test. The results demonstrated that short-term cross-section morphology adjustment is associated with pre-

vious topographic conditions, and the cross-section will be altered for a while to maintain a constant state. In other words, the primary channel may shift while staying the same size. Jiang et al. [91] conducted a generalized physical model test to investigate the process of channel cross-section morphology adjustment due to a unique kind of scour called bottom-block scour, frequently observed in the LYR. The study revealed that the cross-section adjustment displayed clear regularity in four stages, beginning with pre-scour, followed by a relatively stable channel bed elevation, a rapid bed decline due to mud-layered block uplift, and finally, continual scouring followed by back-silting. During the four stages, cross-section morphology adjustment could be classified into the following three types: narrower and deeper, overall undercutting, and local adjustment.

Overall, significant efforts have been dedicated to the morphological adjustment of river cross-sections. These efforts have primarily relied on qualitative analyses of measured data or quantitative assessments of statistical laws through physical modeling tests. Mathematical models have also been employed to study channel siltation or bed deformation, with the morphological adjustment of river cross-sections often being corrected using empirical assumptions. However, there has been limited research into the cross-sectional morphology adjustment based on the principle of water–sediment movement and distribution.

## 5. Discussion

To summarize, there are multiple research findings regarding the lateral distribution of flow velocity and sediment concentration. Empirical formulas based on measured data analysis and theoretical formulas based on the simplification of water and sediment movement equations have been established. Most of these formulas have been tested and applied in practice. However, the empirical formulas lack theoretical grounding, and the theoretical formulas are complex in practical application. Additionally, many existing studies of theoretical formulas have generalized the cross-section morphology to rectangular or trapezoidal shapes, but this oversimplification is insufficient to accurately predict the lateral distribution of flow velocity and sediment concentration in natural rivers of varying morphologies. Furthermore, current studies often only consider longitudinal sediment transport equilibrium; however, in practice, it is almost impossible for both the main channel and its floodplain to satisfy sediment transport equilibrium. Therefore, further exploration is necessary to comprehend the mechanism of the lateral distribution of water and sediment under unbalanced sediment transport conditions in river channels.

Numerous studies also have been conducted on the morphological adjustment of river cross-sections. These studies have mainly consisted of qualitative descriptions of channel evolution processes based on measured data, or quantitative explorations of statistical laws based on mathematical and/or physical models, taking the LYR channel as an example. Despite these efforts, the degree of complexity of river channels still leaves room for further study to fully comprehend the inner mechanisms of cross-section morphology adjustment.

In essence, the irregularity of river cross-sections creates varying water depths along their width, resulting in the uneven lateral distribution of flow velocity and sediment concentration. Consequently, sediment transport capacity is also uneven along the channel width (Equation (8)), which may cause varying degrees of cross-sectional deformation in different locations (Equation (9)). Ultimately, this may trigger the adjustment of cross-sectional morphology.

$$S_* = K \left( \frac{U^3}{gH\omega_s} \right)^M \quad (8)$$

$$\rho' \frac{\partial z}{\partial t} = \omega_s a_* (S - S_*) \quad (9)$$

Equation (8) is a formula for the sediment transport capacity of flow and Equation (9) is used for the calculation of riverbed deformation, where  $K$  and  $M$  are constants and  $\rho'$  is the dry density of bed sediment.  $a_*$  is the saturation recovery coefficient, which is an important

parameter that reflects the rate of recovery of sediment concentration towards saturation, i.e., sediment transport capacity, in the case of non-uniform suspended sediment transport.

It is important for future research to focus more on the lateral distribution mechanism of water and sediment under nonequilibrium sediment transport conditions. Additionally, utilizing the derivation ideas of the lateral distribution equations of flow velocity and sediment concentration, incorporating the sediment transport capacity formula (Equation (8)) and the riverbed deformation equation (Equation (9)), may provide insights into the evolution mechanisms of cross-section morphology from a theoretical perspective on water and sediment movement and distribution. The discoveries related to river channels are crucial for advancing the development of the sediment academic discipline and have practical applications in engineering.

## 6. Summary

To gain a better understanding of how channel morphology adjusts and its complex mechanisms, this paper presents a detailed overview of research findings on overbank flow, sediment transport, and channel morphology in the Lower Yellow River. Moreover, we explore a possible approach to uncovering the evolution of river cross-section morphology from a theoretical standpoint. The main conclusions drawn from this investigation can be summarized as follows:

1. Various empirical and theoretical formulas have been proposed to predict the distribution of lateral depth-averaged flow velocity. These formulas have been established based on data from indoor experiments or on-site measurements, which were used to analyze the characteristics of lateral flow velocity distribution and its influencing factors. Three types of empirical equations have been developed, including exponential, parabolic, and power functions. Additionally, various theoretical formulas have been derived for the lateral distribution of flow velocities. Some of these formulas ignore or simplify the secondary flow term and instead focus on the momentum exchange in the interaction zone between the main channel and its floodplain. Others assume the transverse eddy viscosity coefficient  $\bar{\varepsilon}_{yx} = \lambda U_* H$  and concentrate mainly on the secondary flow term. Despite focusing on different terms, these various formulations offer multiple options for studying the lateral distribution of flow velocities under different flow conditions.
2. The lateral distribution of suspended sediment concentration has not been thoroughly studied due to the challenge of accurately measuring sediment data in rivers and experiments. Nonetheless, there exist both empirical and theoretical formulas that can predict the lateral sediment concentration distribution, similar to the lateral distribution of flow velocity. Considering different factors that influence the lateral distribution of sediment concentration, empirical equations with coefficients determined from the measured data have been proposed. Despite lacking a theoretical foundation, these empirical equations are simple in structure and practical to use. Furthermore, several theoretical formulas have been established via assuming an equilibrium state of longitudinal sediment transport under uniform flow conditions. However, it is important to note that assuming the main channel and its floodplain are simultaneously in an equilibrium state of erosion and siltation is not entirely accurate in reality.
3. Extensive research has been dedicated to examining the morphological adjustments of the LYR channels. These studies typically involve qualitative descriptions of channel evolution processes based on measured data, or quantitative explorations of statistical laws using mathematical and/or physical models. However, there has been limited research on cross-sectional morphology adjustments that utilize the principle of water-sediment movement and distribution. By applying the derivation concepts of lateral distribution equations of flow velocity and sediment concentration, and incorporating the sediment transport capacity formula (Equation (8)) and the riverbed deformation equation (Equation (9)), we may be able to gain theoretical insights into the mechanisms

of cross-section morphology evolution related to water and sediment movement and distribution.

**Author Contributions:** Conceptualization, L.Z. and S.H.; methodology, A.C. and B.L.; software, S.H.; validation, A.C. and J.L.; formal analysis, S.H. and J.W.; investigation, S.H. and L.Z.; resources, S.H. and J.L.; data curation, S.H.; writing—original draft preparation, S.H.; writing—review and editing, S.H., B.L. and J.W.; visualization, S.H.; supervision, L.Z.; project administration, L.Z. and S.H.; funding acquisition, L.Z. and S.H. All authors have read and agreed to the published version of the manuscript.

**Funding:** This study was funded by the National Key R&D Program of China (Grant No. 2023YFC3206202), the National Natural Science Foundation of China (Grant No. 52109086, U2243219 and 52109102), and the Special Project of Basic Scientific Research Business Expenses of Central Public Welfare Research Institutes (Grant No. HKY-JBYW-2022-03).

**Data Availability Statement:** The data presented in this study are available on request from the corresponding author.

**Acknowledgments:** We would like to express our gratitude to the reviewers, editors, and colleagues for their invaluable comments and suggestions, which have significantly improved the manuscript.

**Conflicts of Interest:** Author Baichuan Liu was employed by the company Henan Urban and Rural Planning and Design Research Institute Co., Ltd. The remaining authors declare that the research was conducted in the absence of any commercial or financial relationships that could be construed as a potential conflict of interest.

## References

- Nittrouer, J.A.; Viparelli, E. Sand as a stable and sustainable resource for nourishing the Mississippi River delta. *Nat. Geosci.* **2014**, *7*, 350–354. [[CrossRef](#)]
- Han, S.S.; Rice, S.; Tan, G.M.; Wang, K.R.; Zheng, S. Geomorphic evolution of the Qingshuigou channel of the Yellow River Delta in response to changing water and sediment regimes and human interventions. *Earth Surf. Process. Landf.* **2020**, *45*, 2350–2364. [[CrossRef](#)]
- Makaske, B.; Maathuis, B.H.P.; Padovani, C.R.; Stolker, C.; Mosselman, E.; Jongman, R.H.G. Upstream and downstream controls of recent avulsions on the Taquari megafan, Pantanal, south-western Brazil. *Earth Surf. Process. Landf.* **2012**, *37*, 1313–1326. [[CrossRef](#)]
- Provansal, M.; Dufour, S.; Sabatier, F.; Anthony, E.J.; Raccasi, G.; Robresco, S. The geomorphic evolution and sediment balance of the lower Rhône River (southern France) over the last 130 years: Hydropower dams versus other control factors. *Geomorphology* **2014**, *219*, 27–41. [[CrossRef](#)]
- Wang, B.; Xu, Y.J. Dynamics of 30 large channel bars in the Lower Mississippi River in response to river engineering from 1985 to 2015. *Geomorphology* **2018**, *300*, 31–44. [[CrossRef](#)]
- Abduljaleel, Y.; Munawar, S.; Sarwar, M.K.; Haq, F.U.; Ahmad, K.B. Assessment of River Regime of Chenab River in Post-Chiniot Dam Project Scenario. *Water* **2023**, *15*, 3032. [[CrossRef](#)]
- Zhou, M.R.; Xia, J.Q.; Deng, S.S.; Lu, J.Y.; Lin, F.F. Channel adjustments in a gravel-sand bed reach owing to upstream damming. *Glob. Planet. Chang.* **2018**, *170*, 213–220. [[CrossRef](#)]
- Meade, R.H.; Moody, J.A. Causes for the decline of suspended-sediment discharge in the Mississippi River system, 1940–2007. *Hydrol. Process.* **2010**, *24*, 35–49. [[CrossRef](#)]
- Dai, S.B.; Lu, X.X. Sediment load change in the Yangtze River (Changjiang): A review. *Geomorphology* **2014**, *215*, 60–73. [[CrossRef](#)]
- Wang, H.J.; Wu, X.; Bi, N.S.; Li, S. Impacts of the dam-orientated water-sediment regulation scheme on the lower reaches and delta of the Yellow River (Huanghe): A review. *Glob. Planet. Chang.* **2017**, *157*, 93–113. [[CrossRef](#)]
- Wyźga, B.; Zawiejski, J.; Pawlik, R.A. Impact of channel incision on the hydraulics of flood flows: Examples from Polish Carpathian rivers. *Geomorphology* **2016**, *272*, 10–20. [[CrossRef](#)]
- Smith, N.D.; Morozova, G.S.; Arlucea, M.P.; Gibling, M.R. Dam-induced and natural channel changes in the Saskatchewan River below the E.B. Campbell Dam, Canada. *Geomorphology* **2016**, *269*, 186–202. [[CrossRef](#)]
- Ettema, R.; Armstrong, D.L. Bedload and channel morphology along a braided, sand-bed channel: Insights from a large flume. *J. Hydraul. Res.* **2019**, *57*, 822–835. [[CrossRef](#)]
- Lyu, Y.W.; Fagherazzi, S.; Tan, G.M.; Zheng, S.; Feng, Z.Y.; Han, S.S.; Shu, C.W. Hydrodynamic and geomorphic adjustments of channel bars in the Yichang–Chenglingji Reach of the Middle Yangtze River in response to the Three Gorges Dam operation. *Catena* **2020**, *193*, 104628. [[CrossRef](#)]
- Li, J.; Xia, J.Q.; Kong, L.Z.; Ji, Q.F.; Li, L.L.; Chen, F. Geomorphic adjustments of channel bars in the braided reach of the lower Yellow river from 1986 to 2018. *Catena* **2024**, *236*, 107735. [[CrossRef](#)]

16. Li, J.; Xia, J.Q.; Zhou, M.R.; Deng, S.S.; Wang, Z.H. Channel geometry adjustments in response to hyperconcentrated floods in a braided reach of the Lower Yellow River. *Prog. Phys. Geogr. Earth Environ.* **2018**, *42*, 352–368. [[CrossRef](#)]
17. Zhou, M.R.; Xia, J.Q.; Lu, J.Y.; Deng, S.S.; Lin, F.F. Morphological adjustments in a meandering reach of the middle Yangtze River caused by severe human activities. *Geomorphology* **2017**, *285*, 325–332. [[CrossRef](#)]
18. Zhao, Y.A.; Zhou, W.H.; Fei, X.J. *Basic Law of Channel Evolution in Reaches of the Lower Yellow River*; The Yellow River Water Conservancy Press: Zhengzhou, China, 1998; ISBN 7-80621-148-9.
19. Tang, X.N.; Knight, D.W. A general model of lateral depth-averaged velocity distributions for open channel flows. *Adv. Water Resour.* **2008**, *31*, 846–857. [[CrossRef](#)]
20. Yang, Z.H.; Gao, W.; Huai, W.X. Study on the secondary flow Coefficient of overbank flow. *Appl. Math. Mech.* **2010**, *31*, 681–689.
21. Yang, K.J.; Cao, S.Y.; Knight, D.W. Flow Patterns in Compound Channels with Vegetated Floodplains. *J. Hydraul. Eng.* **2007**, *133*, 148–159. [[CrossRef](#)]
22. Huai, W.X.; Chen, W.X.; Tong, H.Y.; Zhuo, J.M. 3-D numerical simulation on overbank steady open channel flows in compound channels. *Adv. Water Resour.* **2003**, *14*, 15–19.
23. Krishnappan, B.G.; Lau, Y.L. Turbulence modeling of flood plain flows. *J. Hydraul. Eng.* **1986**, *112*, 251–266. [[CrossRef](#)]
24. Shiono, K.; Knight, D.W. Turbulent open channel flows with variable depth across the channel. *J. Fluid Mech.* **1991**, *222*, 617–646. [[CrossRef](#)]
25. Ackers, P. Stage-discharge functions for two-stage channels: The impact of new research. *Water Environ. J.* **1993**, *7*, 52–59. [[CrossRef](#)]
26. Xu, W.L. Study on computational method of overbank flow in channels with compound cross section. *J. Hydraul. Eng.* **2002**, *128*, 21–26+31.
27. Ji, Z.W.; Hu, C.H. Water-sediment movement mechanism in the trough interactive region of compound channels. *Adv. Water Sci.* **2017**, *28*, 321–328. [[CrossRef](#)]
28. Chen, S.L.; Xiao, G.; Zhao, Y.F.; Zhang, J.S.; Wang, W.J. Study on velocity distribution function of river cross section. *J. Hydraul. Eng.* **1999**, *4*, 71–75.
29. Hao, H.K.; He, J.Q.; Lei, X.L. Experimental study on flow measurement and velocity distribution of U-shaped channel section. *China Rural Water Hydropower* **2006**, *8*, 113–115.
30. Luo, T.F.; Lv, H.X.; Zhang, C.J.; Tang, R.P. Study on the lateral velocity distribution and measurement technology of open channel with U-shaped cross section. *China Rural Water Hydropower* **2007**, *10*, 61–64.
31. Sun, D.P.; Wang, E.P.; Dong, Z.H.; Li, G.Q. Discussion and application of velocity profile in open channel with rectangular cross-section. *J. Hydrodyn. Ser. A* **2004**, *2*, 144–151.
32. Han, J.X.; Huang, F.G.; Bian, Y.L.; Wu, Y.L.; Cheng, W.W. Parabolic law for lateral distribution of flow velocity and its application in open channel. *Yellow River* **2013**, *35*, 83–85.
33. Guo, J.B.; Zhu, D.K.; Cheng, X.; Zhu, Y.Z.; Zhang, F. Study on the distribution characteristics of vertical and lateral flow velocity in Lanxi River section. *Sci. Technol. Innov.* **2022**, *11*, 52–54+57. [[CrossRef](#)]
34. Jiang, E.H.; Zhao, L.J.; Zhang, H.W. *Research and Application of Mathematical Model of Flood Evolution and Erosion-Deposition Evolution of Sediment-Laden Rivers*; The Yellow River Water Conservancy Press: Zhengzhou, China, 2008; ISBN 7-80734-179-3.
35. Zhou, Y.L. A study on the transverse distribution of overbank flow velocity. *Eng. J. Wuhan Univ.* **1994**, *27*, 678–684.
36. Chen, L.; Zhan, Y.Z.; Zhou, Y.L.; Wang, M.F. Form and function of water-sediment exchange in floodplain hyperconcentrated flow. *J. Sediment. Res.* **1996**, *02*, 45–49.
37. Xu, W.L.; Knight, D.W.; Tang, X.N. Study on friction factor and eddy viscosity of overbank flows. *Adv. Water Sci.* **2004**, *6*, 723–727.
38. Nokes, R.I.; Wood, I.R. Vertical and lateral turbulent dispersion: Some experimental results. *J. Fluid Mech.* **1998**, *187*, 373–394. [[CrossRef](#)]
39. Zong, H.C.; Jiang, E.H.; Zhao, L.J.; Zhang, X.X. The research of two dimensional analytical solution for overbank flow velocity on the floodplain transverse slope. *Yellow River* **2015**, *37*, 45–49.
40. Wu, T.; Zhang, H.W.; Zhang, H. Transverse distribution of flow velocity in compound channel and its effects on floodplains levees. *J. Hydraul. Eng.* **2009**, *135*, 535–541.
41. Abril, J.B.; Knight, D.W. Stage-discharge prediction for rivers in flood applying a depth-averaged model. *J. Hydraul. Res.* **2004**, *42*, 616–629. [[CrossRef](#)]
42. Wark, J.B. *Discharge Assessment in Straight and Meandering Compound Channels*. Ph.D. Thesis, University of Glasgow, Glasgow, UK, 1993.
43. Irvine, D.A.; Babaeyan-Koopaei, K.; Sellin, R.H.J. Two-dimensional solution for straight and meandering overbank flows. *J. Hydraul. Eng.* **2000**, *126*, 653–669. [[CrossRef](#)]
44. Tang, X.N.; Knight, D.W. Analytical models for velocity distributions in open channel flows. *J. Hydraul. Res.* **2009**, *47*, 418–428. [[CrossRef](#)]
45. Tominaga, A.; Knight, D.W. Numerical evaluation of secondary flow effects on lateral momentum transfer in overbank flows. In *River Flow 2004, Proceedings of the 2nd International Conference on Fluvial Hydraulics, Napoli, Italy, 23–25 June 2004*; CRC Press: Boca Raton, FL, USA, 2004; pp. 353–361.
46. Castanedo, S.; Medina, M.; Mendez, F.J. Models for the turbulent diffusion terms of shallow water equations. *J. Hydraul. Eng.* **2005**, *131*, 217–223. [[CrossRef](#)]

47. Van Prooijen, B.C.; Battjes, J.A.; Uijtewaal, W.S.J. Momentum exchange in straight uniform compound channel flow. *J. Hydraul. Eng.* **2005**, *131*, 175–183. [[CrossRef](#)]
48. Knight, D.W.; Omran, M.; Tang, X.N. Modelling depth averaged velocity and boundary shear in trapezoidal channels with secondary flows. *J. Hydraul. Res.* **2007**, *133*, 39–47. [[CrossRef](#)]
49. Ikeda, S.; McEwan, I.K. *Flow and Sediment Transport in Compound Channels: The Experiences of Japanese and UK Research*; CRC Press: Boca Raton, FL, USA, 2008; ISBN 9789810593636.
50. Knight, D.W. Modelling overbank flows in rivers: Data, concepts, models and calibration. In *Numerical Modelling of Hydrodynamics for Water Resources*; CRC Press: Boca Raton, FL, USA, 2008; pp. 15–36. ISBN 9780429077173.
51. Devi, K.A.B.; Khatua, K.K. Depth-averaged velocity and boundary shear stress prediction in asymmetric compound channels. *Arab. J. Sci. Eng.* **2017**, *42*, 3849–3862. [[CrossRef](#)]
52. Alawadi, W.; Al-Rekabi, W.; Al-Aboodi, A. Application of the Shiono and Knight Model in asymmetric compound channels with different side slopes of the internal wall. *Appl. Water Sci.* **2018**, *8*, 4. [[CrossRef](#)]
53. McGahey, C.; Samuels, P.G.; Knight, D.W. A practical approach to estimating the flow capacity of rivers: Application and analysis. In *Proceedings of the International Conference on Fluvial Hydraulics, Lisbon, Portugal, 6–8 September 2006*; Taylor & Francis: London, UK, 2006; pp. 303–312. [[CrossRef](#)]
54. Rezaei, B.; Knight, D.W. Application of the Shiono and Knight Method in compound channels with non-prismatic floodplains. *J. Hydraul. Res.* **2009**, *47*, 716–726. [[CrossRef](#)]
55. Alawadi, W.; Tumula, P. Depth-averaged simulation of flows in asymmetric compound channels with smooth and rough narrow floodplains. *Australas. J. Water Resour.* **2018**, *22*, 137–148. [[CrossRef](#)]
56. Pu, J.H. Turbulent rectangular compound open channel flow study using multi-zonal approach. *Environ. Fluid Mech.* **2018**, *19*, 785–800. [[CrossRef](#)]
57. Baek, K.O. Deriving Longitudinal Dispersion Coefficient Based on Shiono and Knight Model in Open Channel. *J. Hydraul. Eng.* **2019**, *145*, 06019001. [[CrossRef](#)]
58. Pu, J.H.; Pandey, M.; Hanmaiahgari, P.R. Analytical modelling of sidewall turbulence effect on streamwise velocity profile using 2D approach: A comparison of rectangular and trapezoidal open channel flows. *J. Hydro-Environ. Res.* **2020**, *32*, 17–25. [[CrossRef](#)]
59. Huai, W.X.; Xu, Z.G.; Yang, Z.H.; Zeng, Y.H. Two dimensional analytical solution for a partially vegetated compound channel flow. *Appl. Math. Mech.* **2008**, *29*, 1077–1084. [[CrossRef](#)]
60. Sun, X. Flow Characteristics in Compound Channels with and without Vegetation. Ph.D. Thesis, Loughborough University, Loughborough, UK, 2007.
61. Sun, X.; Shiono, K.; Fu, X.Y.; Yang, K.J.; Huang, T.L. Application of Shiono and Knight Method to Compound Open Channel Flow with One-line Emergent Vegetation. *Adv. Mater. Res.* **2013**, *663*, 930–935. [[CrossRef](#)]
62. Zhang, M.W.; Jiang, C.B.; Huang, H.Q.; Nanson, G.C.; Chen, Z.B.; Yao, W.Y. Analytical models for velocity distributions in compound channels with emerged and submerged vegetated floodplains. *Chin. Geogr. Sci.* **2017**, *27*, 577–588. [[CrossRef](#)]
63. Li, D.; Huai, W.X.; Liu, M.Y. Modeling depth-averaged streamwise velocity in a channel with one-line emergent vegetation patches. *River Res. Appl.* **2022**, *38*, 708–716. [[CrossRef](#)]
64. Gao, Y.H.; Zhang, H.W.; Ma, H.B. Numerical simulation method of alluvial river bed deformation. In *Proceedings of the First Sediment Research Symposium in Henan Province*; The Yellow River Water Conservancy Press: Zhengzhou, China, 1995; pp. 34–39.
65. Wei, Z.L.; Xie, J.H.; Wei, L.Y. *Hydrodynamic Mathematical Model of Flood Forecasting in the Lower Reaches of the Yellow River*; Wuhan University of Hydraulic and Electric Engineering: Wuhan, China, 1990.
66. Zhang, Q.W. Sediment mathematical model of the Lower Yellow River and its calculation. *Yellow River* **1994**, *1*, 4–8.
67. Zhao, L.J.; Jiang, E.H.; Liu, X.S.; Chen, X.C. Study on the lateral distribution of suspended sediment concentration and average particle size. In *Proceedings of the 13th National Hydrodynamics Symposium, Guiyang, China, 9–11 August 1999*; China Ocean Press: Beijing, China, 1999; pp. 424–429.
68. Chen, L.; Wang, M.F.; Zhou, Y.L. Structure of hyperconcentrated flow on floodplain and evolution law of scouring and silting in floodplain and channel. In *Sub-Topic Report on National Key Scientific and Technological Research during the 8th Five-Year Plan Period*; Wuhan University of Hydraulic and Electric Engineering: Wuhan, China, 1995.
69. Liu, B.Y. Study on Sediment Transports and Bed Evolution in Compound Channels. Ph.D. Thesis, Kyoto University, Kyoto, Japan, 1991.
70. Wang, S.Q. Mathematical model scheme calculation of sediment erosion and deposition in reservoirs and lower reaches of the Yellow River. In *Sub-Topic Report on National Key Scientific and Technological Research during the 8th Five-Year Plan Period*; School of Civil Engineering Tsinghua University: Beijing, China, 1995.
71. Shi, C.X.; Xu, J.X. A study on the regularity of adjustment of channel cross-sections and direction of channel training of the Lower Yellow River. *Geogr. Res.* **1997**, *16*, 58–65.
72. Zhang, O.Y.; Xu, J.X.; Zhang, H.W. Impact of flood events from different source areas on channel transects adjustment at the wandering-braided reach of the Lower Yellow River. *J. Sediment. Res.* **2002**, *6*, 1–7.
73. Fu, C.L.; Dong, X.Y.; Han, X.Y.; Ma, X.; Li, Q. Analysis of the change characteristics of river transversal section in downstream of the Yellow River. *J. Water Resour. Water Eng.* **2012**, *23*, 179–181.
74. Li, Y.; Wang, W.H.; Zhang, B.S.; Wang, W.Z. Changes of river regime of the Lower Yellow River Under Long-Term Low-Concentrated Flow Conditions. *Yellow River* **2019**, *41*, 31–35.

75. Zhang, M.W.; Sun, Z.Y.; Peng, H.; Li, Y. Variation characteristic of cross section and its influence to the curvature of bend in the Lower Yellow River. *Yellow River* **2019**, *41*, 24–28.
76. Wang, Y.J.; Wu, B.S.; Zhong, D.Y. Simulating cross-sectional geometry of the main channel in response to changes in water and sediment in Lower Yellow River. *J. Geogr. Sci.* **2020**, *30*, 2033–2052. [[CrossRef](#)]
77. Chen, M.; Xu, L.J.; Xing, C.P.; Xu, H.F.; Zhao, W.J. Analysis of the evolution trends and influential factors of bankfull discharge in the Lower Yellow River. *Sci. Rep.* **2022**, *12*, 19981. [[CrossRef](#)] [[PubMed](#)]
78. Xu, L.J.; Jiang, E.H.; Zhao, L.J.; Li, J.H.; Zhao, W.J.; Zhang, M.W. Research on the Asymmetry of Cross-Sectional Shape and Water and Sediment Distribution in Wandering Channel. *Water* **2022**, *14*, 1214. [[CrossRef](#)]
79. Zhang, X.P.; Jiang, E.H.; Li, J.H.; Zhang, T.K.; Lai, Y.X. A cusp catastrophe model for analyzing sudden channel shifting in wandering reach of the Lower Yellow River. *Sci. Rep.* **2023**, *13*, 17588. [[CrossRef](#)] [[PubMed](#)]
80. Li, X.J. Reach-Scale Analysis Method of Fluvial Processes and Its Application in the Lower Yellow River. Ph.D. Thesis, Wuhan University, Wuhan, China, 2019.
81. Xia, J.Q.; Li, J.; Carling, P.A.; Zhou, M.R.; Zhang, X.L. Dynamic adjustments in bankfull width of a braided reach. *Proc. Inst. Civ. Eng. Water Manag.* **2019**, *172*, 207–216. [[CrossRef](#)]
82. Ni, J.R.; Zhang, H.W.; Xue, A.; Wieprecht, S.; Borthwick, A.G.L. Modelling of hyperconcentrated sediment-laden floods in the LYR. *J. Hydraul. Eng.* **2004**, *130*, 1025–1032. [[CrossRef](#)]
83. Li, W.; Van Maren, D.S.; Wang, Z.B.; de Vriend, H.J.; Wu, B.S. Peak discharge increase in hyperconcentrated floods. *Adv. Water Resour.* **2014**, *67*, 65–77. [[CrossRef](#)]
84. Li, W.; Su, Z.H.; van Maren, D.S.; Wang, Z.B.; de Vriend, H.J. Mechanisms of hyperconcentrated flood propagation in a dynamic channel-floodplain system. *Adv. Water Resour.* **2017**, *107*, 470–489. [[CrossRef](#)]
85. Darby, S.E.; Alabyan, A.M.; Wiel, M.J.V.D. Numerical simulation of bank erosion and channel migration in meandering rivers. *Water Resour. Res.* **2002**, *38*, 2-1–2-21. [[CrossRef](#)]
86. Xia, J.Q.; Wang, G.Q.; Wu, B.S. Mathematical model of longitudinal and transverse deformation of two-dimensional riverbed. *Sci. China Ser. E Technol. Sci.* **2004**, *51*, 165–174.
87. Deng, S.S.; Xia, J.Q.; Zhou, M.R. Coupled two-dimensional modelling of bed evolution and bank erosion in the Upper JingJiang Reach of Middle Yangtze River. *Geomorphology* **2019**, *344*, 10–24. [[CrossRef](#)]
88. Wang, Y.Z.; Xia, J.Q.; Deng, S.S.; Zhou, M.R. Coupled modelling of bank erosion and accretion in the Lower Yellow River. *Adv. Eng. Sci.* **2023**, *55*, 130–141.
89. Wang, M.F.; Chen, L.; Zhou, Y.L. Analysis on Characters and Mechanism of Fluvial Processes of High Sediment-laden Flow in Wandering Channel. *J. Sediment. Res.* **2000**, *1*, 1–6.
90. Zhang, M. The Evolution Characters of the Cross-Section in Lower Yellow River and Discussion of the Adjustment Rule. Master's Thesis, Taiyuan University of Technology, Taiyuan, China, 2006.
91. Jiang, E.H.; Cao, Y.T.; Zhang, Q.; Li, J.H.; Yuan, M.J.; Liu, Y.L. Pattern of channel adjustment due to bottom-block scour on the Yellow River. *Adv. Water Sci.* **2015**, *26*, 509–516.

**Disclaimer/Publisher's Note:** The statements, opinions and data contained in all publications are solely those of the individual author(s) and contributor(s) and not of MDPI and/or the editor(s). MDPI and/or the editor(s) disclaim responsibility for any injury to people or property resulting from any ideas, methods, instructions or products referred to in the content.